journal

J. Am. Ceram. Soc., 1–7 (2013)
DOI: 10.1111/jace.12266

New Sintered Li_2O–Al_2O_3–SiO_2 Ultra-Low Expansion Glass-Ceramic

Viviane O. Soares,[‡,†] Oscar Peitl,[§] and Edgar D. Zanotto[§]

[‡]Department of Science, State University of Maringá, Goioerê, 87360-000, Paraná, Brazil

[§]Vitreous Materials Laboratory, Department of Materials Engineering, Federal University of São Carlos, São Carlos 13565-905, São Paulo, Brazil

We developed a new Li_2O–Al_2O_3–SiO_2 (LAS) ultra-low expansion glass-ceramic by nonisothermal sintering with concurrent crystallization. The optimum sintering conditions were 30°C/min with a maximum temperature of 1000°C. The best sintered material reached 98% of the theoretical density of the parent glass and has an extremely low linear thermal expansion coefficient (0.02×10^{-6}/°C) in the temperature range of 40°C–500°C, which is even lower than that of the commercial glass-ceramic Ceran® that is produced by the traditional ceramization method. The sintered glass-ceramic presents a four-point bending strength of 92 ± 15 MPa, which is similar to that of Ceran® (98 ± 6 MPa), in spite of the 2% porosity. It is white opaque and does not have significant infrared transmission. The maximum use temperature is 600°C. It could thus be used on modern inductively heated cooktops.

I. Introduction

Glass–ceramics of the Li_2O–Al_2O_3–SiO_2 (LAS) system have been extensively investigated and commercialized due to their very low (near zero) thermal expansion coefficient (TEC), excellent thermal shock resistance, high chemical durability, and attractive aesthetics.[1] Cooktop plates for kitchen stoves are the dominant products.[2] They are also used in telescope mirrors and high-temperature furnace windows.[3,4]

Traditionally, glass-ceramics are produced by controlled crystallization of certain glasses, which involves a two-stage heat treatment for nucleation and subsequent crystallization.[5,6] This process requires the addition of proper nucleating agents to the parent glass formulation to promote the formation of crystal nuclei. The most frequently used nucleating agents are TiO_2 and ZrO_2 or their mixture, which is proposed to be more effective.[7]

Glass-ceramics can also be produced via viscous flow sintering of glass particles with concurrent crystallization. The advantage of this process is that the high specific surface area of the fine powders promotes surface crystallization even without the addition of any nucleating agent.[8] However, if the surface crystallization process is rapid, the crystals develop prior to the full densification, and the sintering is hindered. The crystallized surface of the particles does not flow, slowing down the sintering kinetics.[9,10] Unfortunately, glasses of the LAS system exhibit a high tendency for surface crystallization. Therefore, producing high-density sintered LAS glass-ceramics remains a challenge.

Although there are some published works on the sintering of LAS glass-ceramics, the major problem with this process achieving complete densification if a crystallized fraction higher than 60% is desired remains unsolved.[11–19]

A comprehensive review of sintered LAS glass-ceramics is presented in Ref. 20. The previous studies demonstrated that obtaining a dense (99%), low-expansion (TEC < 0.5 ppm/°C) sintered LAS glass-ceramic is not trivial. To the best of our knowledge, a sintered glass-ceramic with these two properties combined has never been reported.

The objective of this study is to obtain a sintered LAS glass-ceramic with a relative density close to one and a thermal expansion coefficient close to zero. The main properties of our sintered GC are compared with the commercial material Ceran® produced by Schott by the traditional method.

II. Experimental Procedure

Several LAS glasses within the chemical composition range (mol%) of 60–70 SiO_2, 10–20 Al_2O_3, 5–10 Li_2O, and 1–4 MgO plus other minor oxides were obtained from analytical-grade chemicals. The mixtures of precursor powders were melted in a platinum crucible at 1600°C for 3 h in an electrical furnace in air. The melts were quenched into water, and the small (~2 mm) pieces of glass were crushed in a high-impact planetary ball mill (Fritsch pulverisette) using an agate jar and agate balls that were 20 mm in diameter. Two distinct size distributions were obtained using the milling conditions: 450 rpm for 60 min and 450 rpm for 60 min followed by 550 rpm for 30 min. These two powders were mixed in a weight ratio of 2:3 to improve the particle packing and, consequently, to maximize the green density of the compacts, as determined by the Alfred model for particle packing[21,22] and experimentally in Ref. 23 The resulting particle size distribution was measured by a laser diffraction particle size analyzer (Horiba–LA930). A high-impact planetary ball mill was employed because it permits a short milling time with considerable reduction in particle size. According to Müller,[24] the reduction of milling time implies particles with a small number of defects per unit area, which can act as nucleation sites (Ns). Consequently, surface crystallization is reduced, and sintering is improved. A conventional horizontal ball mill was employed to obtain a particle size distribution quite similar to that obtained by the planetary ball mill. The milling time used was 34 h, and an agate jar and agate balls of 20 mm in diameter were used. A higher Ns is expected in this case. The ball milling was performed to compare the sinterability of this powder with that of the powder obtained by high-impact milling. The possible use of ball milling was considered because it is the most common industrial milling process.

A Netzsch DSC 404 (Netzsch, Selb, Germany) was employed for determination of the characteristic temperatures (T_g, T_x, and T_m) of the glass powders using a heating rate of 10°C/min.

The number of nucleation sites per unit area (Ns) was measured for the powder obtained by ball milling. A green compact uniaxially pressed at 60 MPa for 15 s was heat treated at 30°C/min up to 860°C and subsequently etched (by

L. Pinckney—contributing editor

Manuscript No. 32388. Received November 30, 2012; approved February 5, 2013.
[†]Author to whom correspondence should be addressed. e-mail: vosoares@uem.br

immersion in 2 vol% HF solution for 15 s) and coated with a thin layer of gold. The heat treatment used was enough to develop easily observable crystals separated from each other. A scanning electron microscope (FEI Magellan 400 L; FEI, Hillsboro, OR) was employed to analyze the partially crystallized surface of the sintered sample. The number of crystals was measured for each micrograph and divided by the considered area using the software ImageJ for image analysis. A total of 13 micrographs were measured.

A hot stage microscope (HSM) (MisuraHSM ODHT–Expert system solutions) was used to sinter a single sample made from each powder: one prepared by ball milling (BM) and the other by planetary milling (PM). Cylindrical samples (diameter 3 mm, height 3.5 mm) were prepared by uniaxial pressing at 25 MPa for 15 s. A constant heating rate of 30°C/min was applied, and images of the samples were captured by a video camera every 2°C. The HSM software analyzed the images automatically and recorded the axial linear shrinkage as a function of temperature. This experiment was carried out to evaluate the effect of milling conditions on the sinterability of the LAS glass-ceramics.

Cylinders (diameter 10 mm, height 4 mm) were produced by uniaxially pressing the glass powders at 65 MPa for 15 s, using 2 wt% of a commercial ceramic binder. The samples were then treated at 500°C for 120 min in an electric furnace to remove the binder. Isostatic pressing at 200 MPa for 60 s was performed (using the powder obtained by PM) to produce samples of dimensions 50 mm × 11 mm × 5 mm.

Sintering was performed in an electric tubular furnace that supported high heating rates. Cylindrical samples, uniaxially pressed as described previously, were heated at 30°C/min until the maximum sintering temperature without any holding time. The samples were cooled down inside the furnace, and the average cooling rate was ~15°C/min. The sintering temperatures employed were 950°C, 1000°C, and 1050°C. In a second experiment, the heating rate was varied in the range of 10°C/min to 80°C/min up to 1000°C to determine the best sintering condition.

After sintering, the samples were ground with SiC abrasive paper and were then polished in a suspension of CeO_2. The porosity of the sintered samples was determined by optical microscopy (Leica DM-RX with a CCD camera DFC 490; Leica, Wetzlar, Germany) and image analysis using the ImageJ software.

The crystalline phases formed in samples sintered at 1000°C and 1050°C were determined by X-ray diffraction (XRD) using a Siemens-D5005 diffractometer (Siemens AG, Munich, Germany), with Cu$K\alpha$ radiation in the 2θ range from 15° to 70° using continuous scans at 2°/min.

Scanning electron microscopy with a secondary electron (SE) detector (SEM, Phillips TMP) was employed to observe the microstructure of polished and etched (by immersion in 2 vol% HF for 15 s) transversal sections of the samples coated with a thin layer of gold.

The thermal expansion coefficient (TEC) was determined using a Netzsch DIL 402 (Netzsch, Selb, Germany) PC dilatometer and a heating rate of 5 K/min in air. Samples of 3 mm × 2 mm ×40 mm were prepared by cutting and polishing to obtain parallel faces. A commercial glass-ceramic produced by Schott by the traditional method of melting and forming followed by internal crystallization (Ceran®) and the sintered glass-ceramics were evaluated.

The flexural strength was measured for the best glass-ceramic developed and the commercial Ceran®. A four-point bending setup with an outer span of 30 mm and an inner span of 10 mm at a crosshead speed of 0.1 mm per 60 s was employed. Six flexure bars (9 mm ×4 mm × 42 mm) for each condition were used for the bending tests. The sample surfaces were ground with 400 mesh SiC paper. This test was performed according to ASTM C158-84.

Thermal shock resistance was also evaluated for the best sintered glass-ceramic. The four-point bending strength was measured for six samples after heating them at 500°C and 600°C and quenching in a bath of water and ice at 0°C (ΔT = 500°C and ΔT = 600°C).

The transmission spectra of the best glass-ceramic, sintered up to 1000°C at 30°C/min, was measured by a UV/VIS spectrometer (Lambda 20; Perkin Elmer, Waltham, MA) in the range 200–1100 nm. A sample 2 mm thick and polished on both surfaces was evaluated.

III. Results

The particle size distributions of some glass powders obtained by high-impact and conventional ball milling are shown in Fig. 1. The glass powders exhibit a bimodal distribution, with maxima at ~0.6 and 6 μm. A quite similar distribution was obtained for both milling processes.

Figure 2 shows the DSC curves of the two glass powders in which the characteristic temperatures can be identified. The glass transition temperature (T_g) is 665°C, and the temperatures of maximum crystallization (T_x) are 893°C and 883°C for the powders obtained in the high-impact grinder and ball mill, respectively, whereas the liquidus temperature (T_m) is ~1240°C for both. A second exothermic peak at 1130°C can be observed. Considering that the particle size distributions are very similar for the two powders, the displacement of T_x indicates a higher Ns for the ball-milled powder.

The parameter Ns for the ball-milled powder was measured by SEM using a total of 13 images similar to that shown in Fig. 3. The average value and standard deviation were $(1.6 \pm 0.8) \times 10^{13}$ crystals/m^2. In a previous work, Ns for the powder obtained by high-impact mill was measured, and its value was $(6 \pm 1) \times 10^{12}$ crystals/m^2.[20]

Figure 4 shows the linear shrinkage, measured by HSM using a heating rate of 30°C/min, for powder compacts obtained by high-impact milling and conventional ball milling. The temperature at which sintering starts is ~780°C, corresponding to the first 1% in linear retraction. The sintering rate, considered as $dL/L_0/dT$, is −0.16% per °C in the temperature range 810°C–884°C and it is identical for both powders. The powders show the same sintering kinetics in the initial stage of sintering (when crystallization is negligible), as expected. The temperatures of sintering saturation are ~884°C and 905°C for the powders obtained by balling milling and high-impact milling, respectively. In the temperature range 910°C–1050°C, no detectable linear retraction was observed.

Compacts from the powder obtained by high-impact milling were sintered at 30°C/min up to 950°C, 1000°C and 1050°C. The porosities measured for each temperature are shown in Table I. Considering that the porosity obtained was only 1.7%, the best sintering temperature was 1000°C. For comparison, a compact of the powder obtained by ball

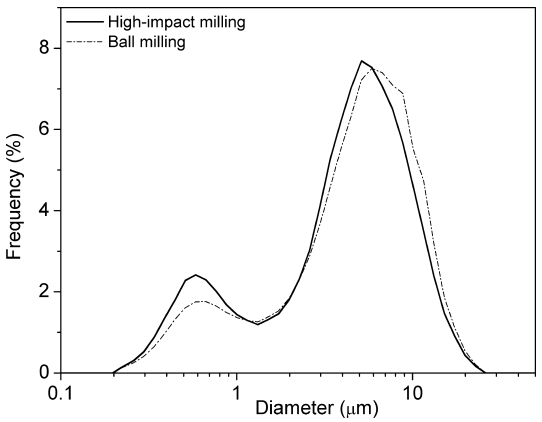

Fig. 1. Particle size distributions of glass powders obtained by high-impact and conventional ball milling.

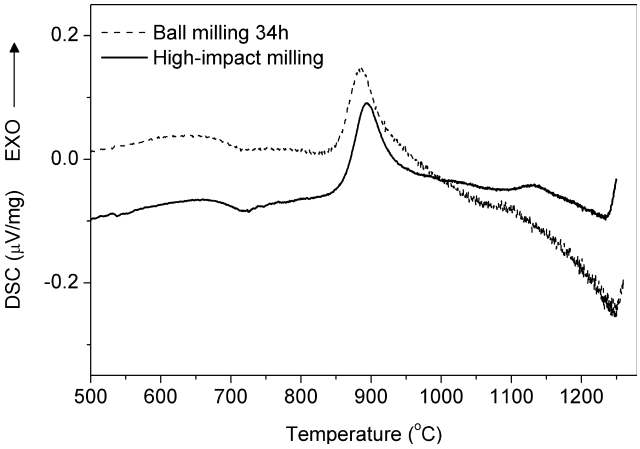

Fig. 2. DSC curves of LAS glass powders obtained by high-impact and conventional ball milling.

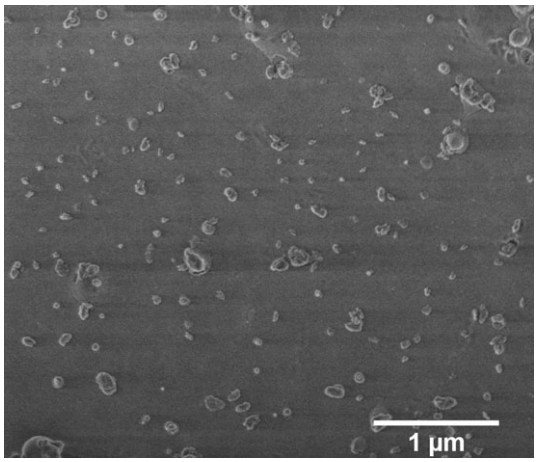

Fig. 3. SEM micrograph of an etched surface from a partially sintered compact heated up to 860°C at 30°C/min. Several crystals can be observed on the glass particle surfaces. The powder was obtained by ball milling.

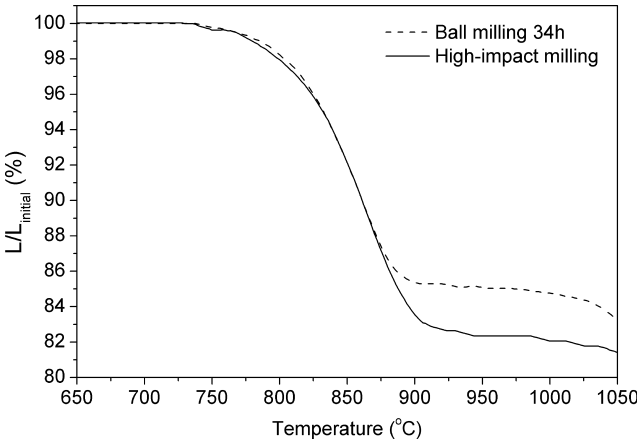

Fig. 4. Linear shrinkage obtained by HSM using a heating rate of 30°C/min comparing two powder compacts: one obtained by high-impact milling and the other by conventional ball milling.

milling was sintered up to 1000°C at 30°C/min, and the residual porosity was 11%.

Figure 5 shows optical micrographs of a polished cross section of an LAS glass-ceramic sintered at 30°C/min up to different temperatures. In Fig. 5(a), irregular pores are observed for a sample sintered up to 950°C; in Fig. 5(b), a highly dense surface can be observed; and in Fig. 5(c), spherical pores with a broad size distribution are observed, which can be related to the degassing, which occurs for sintering at high temperatures. Figure 5(d) shows the compact from the powder obtained by conventional ball milling; irregular pores and a highly porous sample are observed.

Table I. Porosity as a Function of Sintering Temperature Using a Heating Rate of 30°C/min

Powder obtained by	Sintering temperature (°C)	Porosity (%)
High-impact milling	950	7 ± 2
	1000	1.7 ± 0.2
	1050	3.4 ± 0.2
Ball milling	1000	11 ± 2

XRD patterns of an LAS glass-ceramic sintered at 1000°C, 1050°C, and 1000°C with a subsequent heat treatment at 630°C for 912 h are shown in Fig. 6. The crystalline phase formed at 1000°C is Virgilite ($Li_xAl_xSi_{3-x}O_6$) with a β-quartz structure, which is metastable and transforms to β-spodumene ($LiAlSi_2O_6$) at high temperatures.[25] For a sample sintered up to 1050°C, XRD peaks corresponding to β-spodumene can be observed. To evaluate the thermal stability of Virgilite, a sample sintered up to 1000°C was treated at 630°C for 912 h. As shown by Fig. 7 no phase transformation occurs. The application of this material in cooktop panels requires a maximum use temperature of ~600°C, and to ensure a low level of thermal expansion, crystallographic phase transformations must be avoided. Therefore, it is imperative to retain the Virgilite phase during use of this ceramic.

The effect of the powder compaction method on sintering and the surface quality of the GC were evaluated. For compacts obtained by isostatic pressing, a relative green density of 68% ± 2% was obtained, whereas for compacts obtained by uniaxial pressing, this value was only 60% ± 2%. Samples produced by uniaxial and isostatic pressing, sintered in the same condition, are compared in Fig. 8. As seen in Fig. 8(a), uniaxial pressing leads to defects, such as density gradients, especially in large samples (60 mm × 20 mm × 4 mm). The main advantages of isostatic pressing observed in this study were a high green density, homogeneity, and reproducibility of the compact.

The porosity as a function of heating rate for sintered GCs is shown in Fig. 9. The maximum sintering temperature was achieved at 1000°C. Higher temperatures were not used to avoid the formation of the undesired phase β-spodumene, which has a positive TEC. Heating rates of 10°C/min to 80°C/min were employed and, as seen in Fig. 9, the optimum sintering heating rate is ~30°C/min.

The microstructures of all the sintered glass-ceramics (1000°C; 30°C/min) consist of large glass portions ("glass islands") and smaller rounded Virgilite crystals embedded in a residual glass, as observed in Fig. 10. During the sintering process, the particle surface crystallizes, and crystal impingement creates a crystallized layer in each particle. The coarse particles remain vitreous inside. This can be visualized in Fig. 10(a), in which portions of residual glass are indicated by arrows. Figure 10(b) shows a relatively broad size distribution of crystals. Their morphology is mostly spherical, and due the high crystallized fraction, most crystals are in contact with their neighbors. In a previous work, the crystalline volume fraction of Virgilite for this same heat treatment was estimated from the Rietveld refinements of a 1–1 mixture by weight of alumina and sintered glass-ceramic powder. It was found to be 84.1% ± 0.3% Virgilite, 4.6% ± 0.2% an extra crystalline phase attributed to β-spodumene and 11% a residual glassy phase.[26]

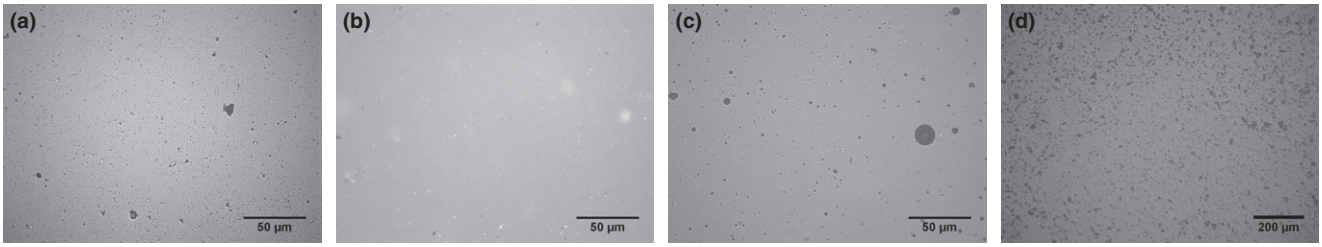

Fig. 5. Optical micrographs of polished cross sections of an LAS glass-ceramic sintered at 30°C/min up to: (a) 950°C, (b) 1000°C, (c) 1050°C and (d) 1000°C for a compact from the powder obtained by conventional ball milling.

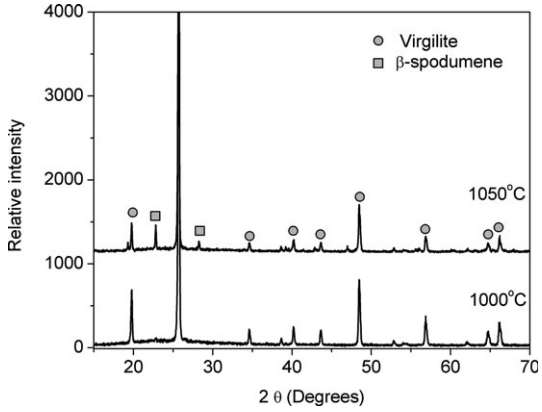

Fig. 6. XRD patterns of an LAS glass-ceramic sintered at 1000°C and 1050°C. Circles: hexagonal Virgilite ($Li_xAl_xSi_{3-x}O_6$; $0.5 < x < 1$) JCPDS 31-0707; squares: tetragonal β-spodumene ($LiAlSi_2O_6$) JCPDS 35-0794.

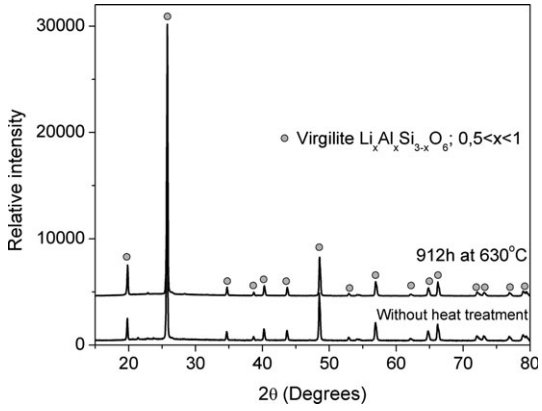

Fig. 7. XRD patterns of an LAS glass-ceramic sintered at 1000°C and the same glass-ceramic heat treated at 630°C for 912 h.

The sintered glass-ceramic shows a higher dimensional stability up to 600°C compared with the commercial Ceran®, as seen in Fig. 11. The TEC of Ceran® is -0.3 × 10^{-6}/°C, (measured in the temperature interval 40°C–500°C), whereas the TEC of our best sintered LAS glass-ceramic is 0.02 × 10^{-6}/°C. However, Ceran® withstands a higher use temperature; its softening point is approximately 700°C. For our sintered glass-ceramic, the residual glass starts to flow at ~650°C, as shown in Fig. 11 by the change in the slope of the thermal expansion curve.

The measured four-point bending strength is 98 ± 6 MPa for Ceran® and 92 ± 15 MPa for the sintered LAS glass-ceramic. These values are quite similar when taking the standard deviation into account. Figure 12 shows that the mechanical strength of sintered LAS glass-ceramic is unchanged after the samples are submitted to a thermal shock treatment up to 600°C. This behavior indicates an excellent thermal shock resistance for this new sintered glass-ceramic.

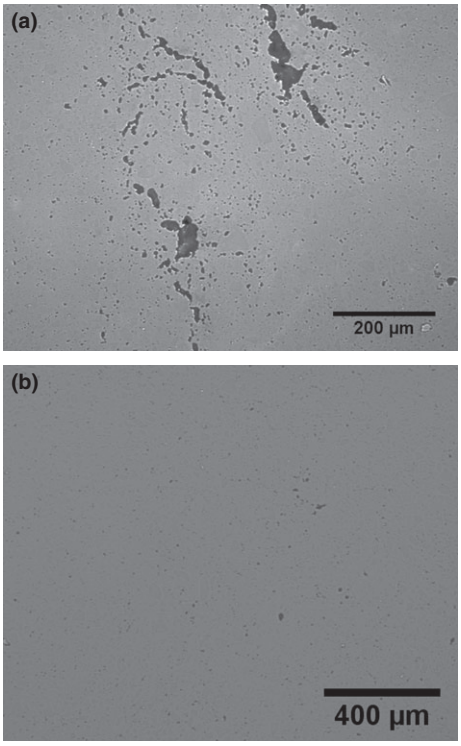

Fig. 8. Optical micrograph of a polished cross section of LAS glass-ceramic sintered at 30°C/min up to 1000°C: (a) uniaxial pressing at 65 MPa; (b) isostatic pressing at 200 MPa.

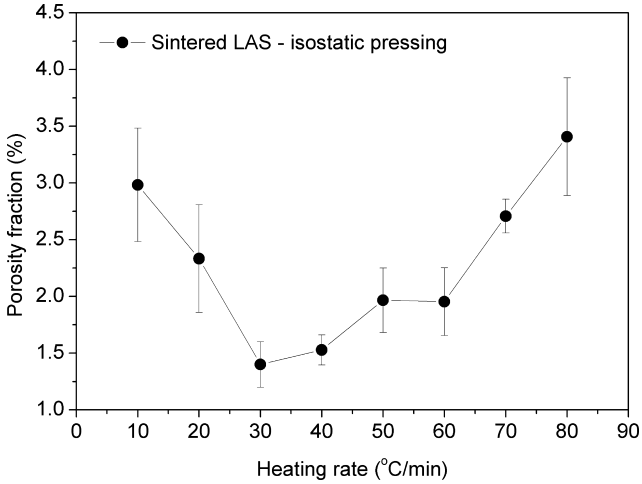

Fig. 9. Porosity as a function of heating rate for LAS glass-ceramics sintered up to 1000°C.

Glass-ceramics used in electrical cooktops with an electrical resistance wire must meet specific transmission specifications in the visible (to be nearly opaque) and in the near IR

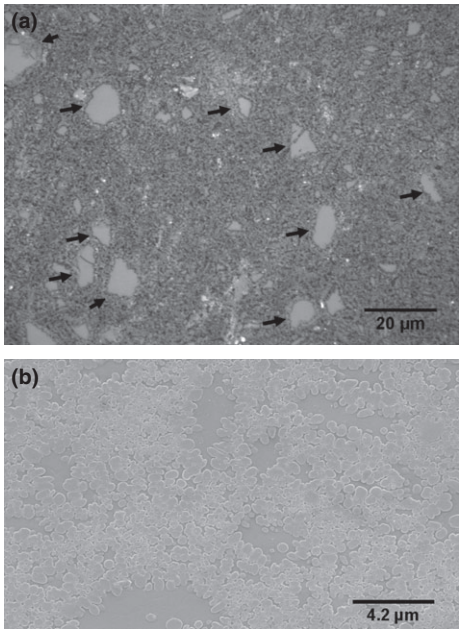

Fig. 10. Polished and etched cross section of an LAS glass-ceramic sintered up to 1000°C at 30°C/min: (a) optical micrograph and (b) SEM micrograph.

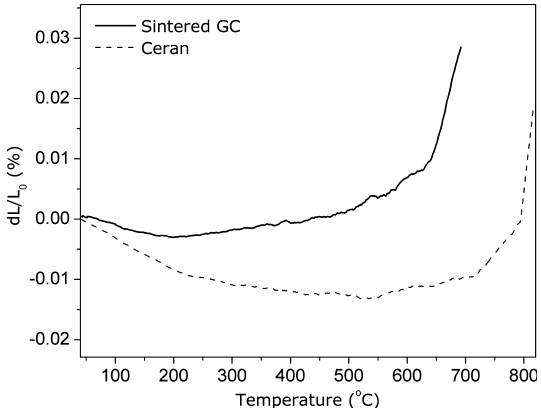

Fig. 11. Linear thermal expansion curves of our sintered glass-ceramic and the commercial glass-ceramic Ceran®.

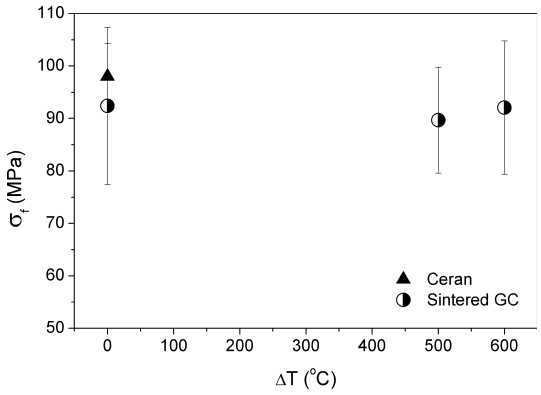

Fig. 12. Four-point flexural strength as a function of the thermal shock temperature of the sintered glass-ceramic and Ceran®. For each point, six samples were probed.

(to be transparent) spectral regions. A typical transmission in the IR for the commercial glass-ceramic is approximately 80%. The developed sintered glass-ceramic does not present a significant IR transmission, as seen in Fig. 13, and thus may be used only in inductively heated cooktops.

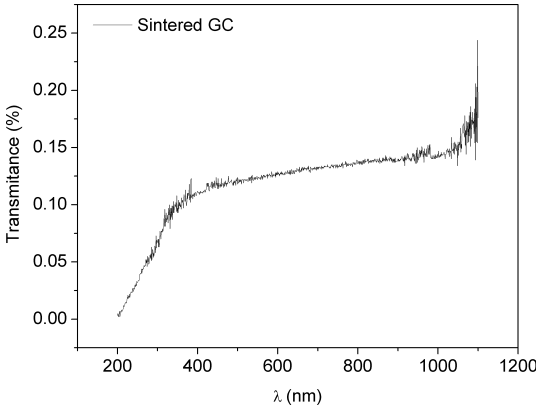

Fig. 13. Infrared transmittance of the sintered glass-ceramic.

IV. Discussion

Conventional ball milling is not an adequate grinding procedure for the LAS glass-ceramic developed here. The milling time required to obtain a similar PSD is extremely high (34 h) when compared with high-impact milling (90 min), and the resulting Ns is quite high, impairing its sinterability. According to Müller,[24] appropriate milling of glass powders, such as the use of short milling times, can improve sinterability due to less numerous crystal nucleation sites at the powder surface. Short milling times are associated with a lower Ns, which favors viscous flow over crystallization. The PSD obtained by ball milling is similar to that obtained by high-impact ball milling (Fig. 1). However, when sintered at the same conditions, the powder obtained by ball milling does not sinter, and its porosity is ~6.5 times higher than the powder obtained by high-impact milling [Fig. 5(d)].The poor sinterability of the powder obtained by ball milling is clearly due to its higher Ns. The premature crystallization of particle surfaces, as can be observed by the exothermic peak in DSC (Fig. 2), hinders sintering by viscous flow.

The evolution of porosity as a function of sintering temperature at a heating rate of 30°C/min is shown in Fig. 3 for the powder obtained by high-impact planetary ball milling. At 950°C, the pores have an irregular shape, and the maximum densification was not reached. At 1000°C, a few pores stay inside the sample and maximum densification is observed. At 1050°C, spherical pores are observed, and the porosity significantly increases. The change in the pore pattern at higher temperatures can be explained by the reduction in the residual glass viscosity. The air inside the pores tends to expand, and the low residual glass viscosity allows the pore to become spherical. The degassing during further crystallization raises the porosity, and new pores are formed. To improve densification, sintering temperatures higher than 1000°C must be avoided.

Isothermal heat treatments at temperatures above 900°C, especially at the maximum sintering temperature, lead to the crystallization of phases of positive TEC and degassing (due to excessive crystallization). These facts justify the sintering heat treatment employed in this work: no subsequent heat treatment is performed to promote further crystallization. Spherical pores and a high crystallized fraction can be observed in Fig. 14, which shows an LAS glass-ceramic sintered up to 1080°C and subsequently heat treated at 980°C for 20 min.

The main phase formed in the sintered glass-ceramic is Virgilite. It has a stuffed β-quartz structure, and it crystallizes as a metastable phase, which tends to transform into β-spodumene at higher temperatures. β-spodumene can be

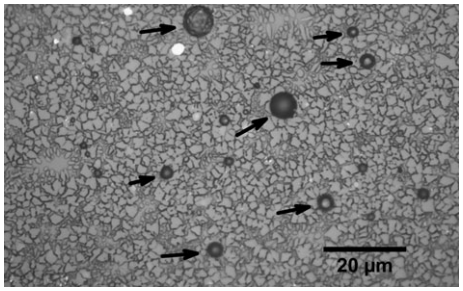

Fig. 14. Optical micrograph of the polished and etched surface of an LAS glass-ceramic sintered at 30°C/min up to 1080°C and heat treated at 980°C for 20 min. The arrows indicate spherical pores formed due to degassing.

observed in a sample sintered up to 1050°C, as shown in Fig. 6. Virgilite possesses a negative TEC (-1.3×10^{-6}/°C), as determined in a previous work.[26] Consequently, it can decrease the TEC of glass-ceramics dramatically, allowing values near zero. β-spodumene has a positive TEC (0.9×10^{-6}/°C), and its formation can be avoided in the developed glass-ceramic for sintering temperatures up to 1000°C. The thermal stability of Virgilite was observed up to 630°C, which can be considered the temperature of application for the sintered glass-ceramic.

The Clusters model of sintering[27] predicts that high heating rates improve the sintering of crystallizing glass particles because crystallization is shifted to higher temperatures. However, because the sintering treatments used in this work are nonisothermal, the use of excessively high rates may result in porous bodies because the treatment time becomes insufficient for sintering and the compact does not follow the heating rate of the furnace. The optimum heating rate determined is 30°C/min, as shown in Fig. 8. For lower heating rates, the surface crystallization happens in the initial stages of sintering, hindering viscous flows, and some pores stay in the compact, resulting in a high porosity. For heating rates higher than 30°C/min, the temperature increases so rapidly that the porous glassy powder compact, which has a low thermal conductivity, does not follow the furnace temperature and, consequently, does not reach the necessary temperature to sinter completely.

The higher dimensional stability of the sintered glass-ceramic up to 600°C compared with the commercial Ceran® is shown in Fig. 10. The near-zero expansion is due to the balanced proportions of crystals and the residual glass phase. Virgilite has a negative TEC, which combined with a residual glass with a positive TEC, gives the overall TEC of the glass-ceramic. The volume fraction of Virgilite in our best sintered glass-ceramic is 84%, whereas in Ceran®, this value is ~70%.[26] However, the residual glasses of these glass-ceramics are not identical. The calculated TEC of the residual glasses applying the mixture rule are $\sim 7 \times 10^{-6}$/°C for sintered GC and 2×10^{-6}/°C for Ceran®. The presence of microcracks, studied in a previous work,[26] can also alter the expansion behavior of our sintered glass-ceramic. This reduction in the apparent thermal expansion due to grain-boundary microcracking has been observed for magnesium and aluminum titanate ceramics.[28,29]

The service temperature of any glass-ceramic is limited by the softening temperature of the residual glass phase. Some differences in the residual glass composition are responsible for the higher softening temperature of Ceran®, which is 50°C higher than the sintered LAS glass-ceramic.

Although our sintered glass-ceramic presents residual porosity and "glass islands" in its microstructure, the value of its bending strength is quite similar to that of Ceran®. The thermal shock resistance of the sintered glass-ceramic is maintained up to 600°C.

The extremely low infrared transmittance in the sintered glass-ceramic can be explained by the scattering of pores and crystals with sizes up to 2 μm. Nevertheless, the developed glass-ceramic can be applied in inductively heated cooktops.

V. Conclusions

A nonisothermal sintering process with concurrent crystallization of an adequate glass powder compact has been successfully developed for the production of an ultra-low TEC glass-ceramic of the LAS system.

The use of conventional ball milling is prohibited in this process due to the significant increase in the number of the nucleation sites, which promotes surface crystallization and hinders viscous flow sintering. The sintering temperature of our glass is limited to 1000°C due to the formation of β-spodumene, which has a positive TEC, and also due to degassing which increases the porosity of the glass-ceramic. The optimum heating rate for our material was 30°C/min.

The best sintered glass-ceramic developed shows a residual porosity of only 1.4%, a near-zero TEC (0.02×10^{-6}/°C) in the temperature range 40°C–500°C and a bending strength similar to that of the commercial glass-ceramic Ceran®. It is white opaque and lacks infrared transmission. The maximum use temperature is 600°C, and it has an excellent thermal shock resistance up to this temperature. Its softening point is ~650°C. These characteristics emphasize the potential application of the present sintered glass-ceramic in induction cooktop surfaces.

References

[1]G. H. Beall, "Design and Properties of Glass-Ceramics," *Annu. Rev. Mater. Sci.*, **22**, 91–119 (1992).
[2]W. Pannhorst, "Recent Developments for Commercial Applications of Low Expansion Glass Ceramics," *Glass Technol.*, **45** [2] 51–3 (2004).
[3]W. Pannhorst, "Glass Ceramics: State of the Art," *J. Non-Cryst. Solids*, **219**, 198–204 (1997).
[4]G. Muller, "The Scientific Basis"; pp. 13–49 in *Low Thermal Expansion Glass-Ceramics*, Edited byH. Bach. Springer-Verlag press, Berlin, 1995
[5]W. Pannhorst. "Overview"; pp. 1–12 in *Low Thermal Expansion Glass-Ceramics*, H. Bach. Springer-Verlag press, Berlin, 1995
[6]E. D. Zanotto, "A Bright Future for Glass-Ceramics," *Am. Ceram. Soc. Bull.*, **89** [8] 19–27 (2010).
[7]M. Tashiro, "Crystallization of Glasses: Science and Technology," *J. Non-Cryst. Solids*, **73**, 575–84 (1985).
[8]R. Müller, E. D. Zanotto, and V. M. Fokin, "Surface Crystallization of Silicate Glasses: Nucleation Sites and Kinetics," *J. Non-Cryst. Solids*, **274** [1–3] 208–31 (2000).
[9]M. O. Prado and E. D. Zanotto, "Glass Sintering with Concurrent Crystallization," *C. R. Chimie*, **5**, 773–86 (2002).
[10]T. J. Clark and S. J. Reed, "Kinetics Process Involved in the Sintering and Crystallization of Glass Powder," *J. Am. Ceram. Soc.*, **69** [11] 837–46 (1986).
[11]S. Knickerbocker, M. R. Tuzzolo, and S. Lawhorne, "Sinterable β-Spodumene Glass-Ceramics," *J. Am. Ceram. Soc.*, **72** [10] 1873–9 (1989).
[12]Y. M. Sung, "Mechanical Properties of α-Cordierite and β-Spodumene Glass-Ceramics Prepared by Sintering and Crystallization Heat Treatments," *Ceram. Int.*, **23**, 401–7 (1997).
[13]Y. M. Sung, S. A. Dunn, and J. A. Koutsky, "The Effect of Boria and Titania Addition on the Crystallization and Sintering Behavior of Li_2O-Al_2O_3-$4SiO_2$ Glass," *J. Eur. Ceram. Soc.*, **14**, 455–62 (1994).
[14]M. C. Wang, S. Yang, S. B. Wen, and N. C. Wu, "Sintering Li_2O–Al_2O_3–$4SiO_2$ Precursor Powders with Ultrafine TiO_2 Additives," *Mater. Chem. Phys.*, **76**, 162–70 (2002).
[15]M. C Wang, N. C. Wu, S. Yang, and S. B. Wen, "Morphology and Microstructure in the Sintering of β-Spodumene Precursor Powders with TiO_2 Additive," *J. Eur. Ceram. Soc.*, **23**, 437–43 (2003).
[16]M. Guedes, A. C. Ferro, and J. M. F. Ferreira, "Nucleation and Crystal Growth in Commercial LAS Compositions," *J. Eur. Ceram. Soc.*, **21** [9] 1187–94 (2001).
[17]P. Riello, S. Bucella, L. Zamengo, U. Anselme-Tamburini, R. Francini, S. Pietrantoni, and Z. A. Munir, "Erbium-Doped LAS Glass-Ceramics Prepared by Spark Plasma Sintering (SPS)," *J. Eur. Ceram. Soc.*, **26**, 3301–6 (2006).
[18]E. I. Suzdal'tsev and D. V. Kharitonov, "Intensified Sintering of Lithiumaluminosilicate Ceramics," *Refract. Ind. Ceram*, **45** [2] 88–90 (2004).
[19]E. I. Suzdal'tsev, "Effect of Temperature on the Structuring and Properties of Glass and Glass Ceramic of Lithium Aluminosilicate Composition," *Refract. Ind. Ceram*, **43** [3–4] 127–35 (2002).
[20]V. O. Soares, R. M. Reis, E. D. Zanotto, M. J. Pascual, and A. Durán, "Non-Isothermal Sinter-Crystallization of Jagged Li_2O-Al_2O_3-SiO_2 Glass and

Simulation Using a Modified Form of the *Clusters* Model," *J. Non-Cryst. Solids*, **358** [23] 3234–42 (2012).

[21]J. E. Funk and D. R. Dinger, "Particle Packing, Part 1 – Fundamentals of Particle Packing Monodisperse Spheres," *Interceram.*, **41** [1] 10–4 (1992).

[22]R. G. Pileggi, F. Ortega, R. Morábito, S. Vendrasco, and V. C. Pandolfelli, "Development and Application of a Software Designed to Combine Different Raw Materials in Order to Obtain Ceramic Products," *Cerâmica*, **44** [289] 189–95 (1998).

[23]V. O. Soares, "Synthesis of Li_2O-Al_2O_3-SiO_2 (LAS) Glass-Ceramics by Sintering with Concurrent Crystallization"; MSc Dissertation (Master's degree in Materials Science and Engineering), Federal University of São Carlos, Brazil, 2007. (in Portuguese).

[24]R. Müller, S. Reinsch, and M. Gaber, "Sinterability of Glass Powders," *Gl. Sci. T. – Gl.*, **73** [C1] 205–12 (2000). (International Symposium on Crystallization in Glasses and Liquids, Vaduz, Switzerland)

[25]O. A. Al-Harb, "Effect of Different Nucleation Catalysts on the Crystallization of Li_2O-ZnO-MgO-Al_2O_3-SiO_2 Glasses," *Ceram. Int.*, **35**, 1121–8 (2009).

[26]F. C. Serbena, V. O. Soares, O. Peitl, H. Pinto, R. Muccillo, and E. D. Zanotto, "Internal Residual Stresses in Sintered and Commercial Low Expansion Li_2O-Al_2O_3-SiO_2 Glass-Ceramics," *J. Am. Ceram. Soc.*, **94** [4] 1206–14 (2011).

[27]M. O. Prado, C. Fredericci, and E. D. Zanotto, "Non-Isothermal Sintering with Concurrent Crystallization of Polidispersed Soda-Lime-Silica Glass Beads," *J. Non-Cryst. Solids*, **331**, 157–67 (2003).

[28]L. Giordano, M. Viviani, C. Bottino, M. T. Buscaglia, V. Buscaglia, and P. Nanni, "Microstructure and Thermal Expansion of Al_2TiO_5–$MgTi_2O_5$ Solid Solutions Obtained by Reaction Sintering," *J. Eur. Ceram. Soc.*, **22**, 1811–22 (2002).

[29]Y. Ohya and Z. Nakagawa, "Grain-Boundary Microcracking Due to Thermal Expansion Anisotropy in Aluminum Titanate Ceramics," *J. Am. Ceram. Soc.*, **70** [8] C184–6 (1987). □